

UNCLASSIFIED

Defense Technical Information Center
Compilation Part Notice

ADP011114

TITLE: Shock Control by Adaptive Elements for Transportation Aircraft Wings

DISTRIBUTION: Approved for public release, distribution unlimited

This paper is part of the following report:

TITLE: Active Control Technology for Enhanced Performance Operational Capabilities of Military Aircraft, Land Vehicles and Sea Vehicles
[Technologies des systemes a commandes actives pour l'amelioration des performances operationnelles des aeronefs militaires, des vehicules terrestres et des vehicules maritimes]

To order the complete compilation report, use: ADA395700

The component part is provided here to allow users access to individually authored sections of proceedings, annals, symposia, etc. However, the component should be considered within the context of the overall compilation report and not as a stand-alone technical report.

The following component part numbers comprise the compilation report:

ADP011101 thru ADP011178

UNCLASSIFIED

SHOCK CONTROL BY ADAPTIVE ELEMENTS FOR TRANSPORTATION AIRCRAFT WINGS

H. Rosemann, J. Birkemeyer, and A. Knauer

Institut für Strömungsmechanik
Deutsches Zentrum für Luft- und Raumfahrt e. V.
Bunsenstr. 10, D-37073 Göttingen, Germany

ABSTRACT

Different devices for the application of shock and boundary layer control on transportation aircraft wings have been investigated on 2-d airfoils and on a swept wing model. A cavity in the surface underneath the foot of the shock covered with a perforated plate reduces shock strength and hence wave drag, but viscous drag increases such that a net drag reduction can not be achieved in most cases. The application of additional boundary layer suction reduces the additional viscous drag, but not enough to result in a significant gain in total drag.

On the contrary a contour bump underneath the shock, applied alone or in combination with suction, reduces very effectively wave drag without increasing viscous drag so that under off-design conditions up to 24% total drag reduction has been measured for a 2-d airfoil and somewhat lower values for the swept wing. This effect has been well predicted by numerical methods. Both devices, especially the perforation, have a positive influence on the buffet boundary.

Trailing edge devices such as conventional and Gurney-type flaps also effect wave drag by redistributing the pressure on the wing or airfoil. Combining them with a contour bump has been investigated numerically. The results show that by careful optimization of the flap deflection together with the corresponding bump location and height a better performance can be achieved compared to the application of either device alone.

NOMENCLATURE

Symbols

b	Span
c	Chord length
c_p	Pressure coefficient
c_D	Drag coefficient
c_{DV}	Viscous drag coefficient
c_{DW}	Wave drag coefficient
c_L	Lift coefficient
c_Q	Suction coefficient
h	Bump height
M	Mach number
p	Pressure
p_0	Total pressure
Re	Reynolds number
x	Streamwise coordinate
z	Normal coordinate

Greek Symbols

α	Model angle of attack
----------	-----------------------

1 INTRODUCTION

The conventional design of a transportation aircraft wing is usually optimized for a given cruise flight operating point. Changing flight parameters, e.g. speed, altitude or weight, often im-

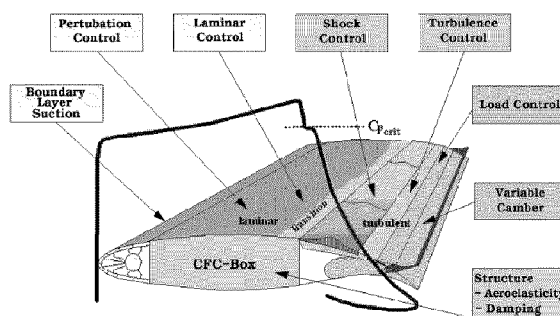


Figure 1: Flow control methods for application on the Adaptive Wing

plies a significant degradation of wing performance. Applying adaptive elements may increase the flexibility of a wing design by significantly reducing the cost of operating at off-design conditions.

Figure 1 shows a number of control devices attributed to the Adaptive Wing Technology. Besides the techniques directly acting on the boundary layer, the most effective methods are the global redistribution of the pressure by trailing edge devices (flaps, flexible trailing edge, Gurney flaps) and the local control of the shock to minimize wave drag (passive or active ventilation, contour bumps). These techniques can be utilized to extend the flight envelope to higher velocities, where it is usually limited by the increase of wave drag and shock induced separation caused by strong shocks.

The investigation of shock control by adaptive elements has been a major topic of the research activities in this field at the DLR Institute of Fluid Mechanics during the last years. First experiments started with the application of a perforated surface with a cavity underneath in the region where the shock impinges on the surface of the airfoil. This device was not very successful in reducing total drag; however, the results suggested that by replacing the ventilation by a solid contour bump a much better performance should be achievable.

Systematic experimental and numerical investigations were then undertaken in the framework of the EU-program EuroShock II and the German adaptive wing research program ADIF to study the underlying flow phenomena, optimize bump geometry and position and demonstrate the drag reductions achievable. To determine the additional effect of the 3-d boundary layer of a typical transonic wing on the shock/boundary layer interaction, the investigations included 2-d airfoils as well as a swept wing model.

The paper discusses some results obtained during these research programs for the application of the control devices alone and in combination with additional boundary layer suction. Recently,

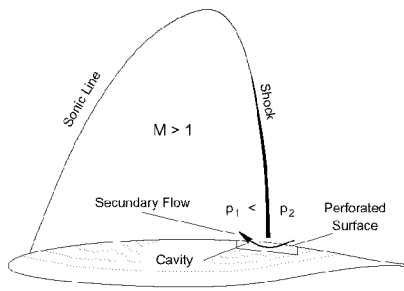


Figure 2: Passive ventilation for shock control

an optimization study on a combined application of a contour bump together with a flexible trailing edge has been performed and results will be shown together with first experiments on airfoils with Gurney flaps at transonic speed.

2 SHOCK CONTROL ON AIRFOILS BY A PERFORATED SURFACE

As outlined above, first attempts to reduce shock strength and thus wave drag were made with a cavity in the surface of the airfoil under the shock position covered by a perforated plate. The basic set-up is sketched in Fig. 2

A secondary flow is established in the cavity driven by the pressure rise across the shock effectively creating a “pneumatic bump” by modulating the boundary layer displacement thickness when the flow exits the cavity in front of the shock and re-enters behind it. Compression waves emanating from the rising slope of the bump hit the shock, weaken it and thus reduce wave drag.

The details of the flow field in the region of the shock/boundary layer interaction above the cavity have been investigated in a channel flow by Bur *et al.*, Ref. 1, both experimentally and numerically. Their results show, that the single shock is indeed replaced by a lambda shock system, thus reducing wave drag. At the same time, however, the boundary layer thickness increases substantially due to the additional losses in the flow through the perforation such that viscous drag is increased.

These effects can be clearly identified also in Fig. 3, where passive ventilation was applied on the laminar-type airfoil LVA-1, tested in the 0.4 m × 0.35 m DLR Cryogenic Ludwig Tube (KRG) in Göttingen (Ref. 2, Ref. 5). As a result of the spreading of the shock the pressure gradient in the shock region is significantly reduced, when the perforation is open. The increase

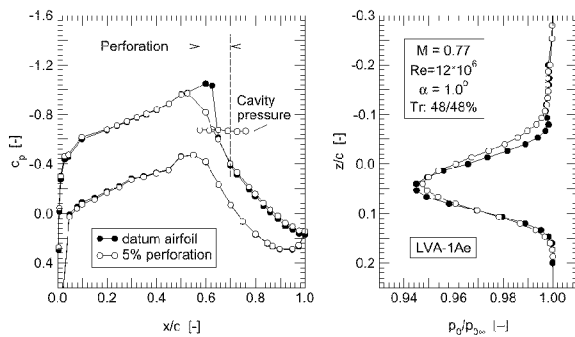


Figure 3: Surface and wake pressure distributions on the laminar-type airfoil LVA-1Ae with and without passive control

of the displacement thickness of the boundary layer shows up in the wake pressure distribution and in the lower trailing edge pressure. The additional viscous drag is higher than the reduction of wave drag such that total drag is increasing by 9% in this case.

A total drag increase has been found in all cases for laminar-type airfoils. Under certain conditions, slight gains in total drag were found for turbulent airfoils, but in general it had to be accepted that passive ventilation can not be applied successfully for drag reduction. An additional suction slot upstream of the interaction region reduces the drag increase, but not to the point where significant reductions are achieved.

Passive ventilation can, however, be applied successfully for reducing shock induced separation. The pressure distribution in Fig. 4 was obtained from an experiment on the VA-2 airfoil tested in the 1 m × 1 m DLR Transonic Wind Tunnel Göttingen (TWG), Ref. 5.

The curves indicate for the closed surface a strong separation with an oscillating shock, as can be deduced from the spread of the pressure distribution in the shock region. When the cavity is opened, the shock strength is reduced, the flow stabilizes and the separation disappears. In this special case, drag is obviously also reduced by a large amount.

3 SHOCK CONTROL ON AIRFOILS BY CONTOUR BUMPS

The logical conclusion from the results reported above was to replace the cavity and the perforation by a solid bump in the surface of the airfoil or wing, thereby maintaining the positive effect on the shock without having to accept the increase of viscous drag. The following investigations were supported by the EU-program EuroShock II and represent the key aerodynamic element in the cooperation between DaimlerChrysler Aerospace Airbus, DaimlerChrysler Forschung and DLR cooperation on adaptive wing technologies, ADIF.

First, an extensive numerical study was carried out to determine the optimum values for the geometric parameters of the bump, as there are: shape, extension, position and height. It was found, that for best performance the length of the bump should be around 20% chord and the shape asymmetric with the maximum height at about 60% of the length of the bump without discontinuities in the contour, *cf.* Ref. 4. While these parameters are not very critical, the position of the crest of the bump and the height have to be very carefully adjusted to the position and strength of the shock.

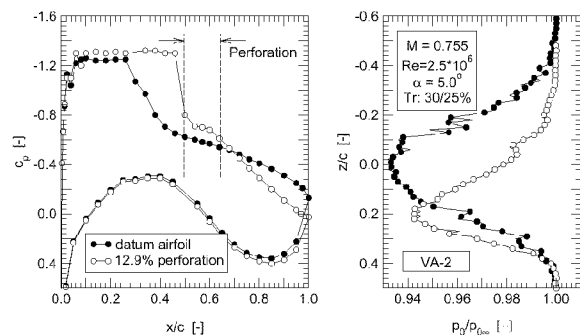


Figure 4: Surface and wake pressure distributions on the turbulent-type airfoil VA-2 with and without passive control

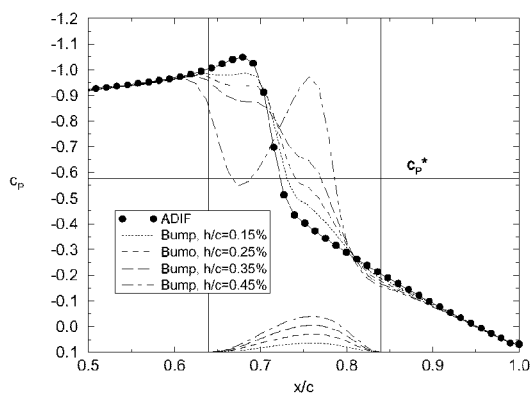


Figure 5: Calculated pressure distribution in the shock region of the ADIF airfoil for different bump heights for $M = 0.755$

Figure 5 shows a result of the pressure distribution in the shock region calculated for different bump heights on the ADIF airfoil. While initially the effect of a reduction of the pressure gradient of the shock increases with increasing bump height, the last curve for the highest bump exhibits a double shock configura-

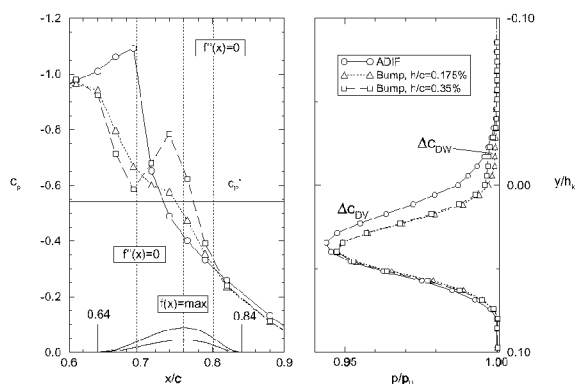


Figure 7: Measured pressure distribution in the shock region of the ADIF-airfoil for different bump heights for $M = 0.765$

tion with a significant drag increase. Obviously the optimum bump height depends on the shock strength, while the position has to follow the shock such that the relative distance between bump maximum and shock position is maintained about constant.

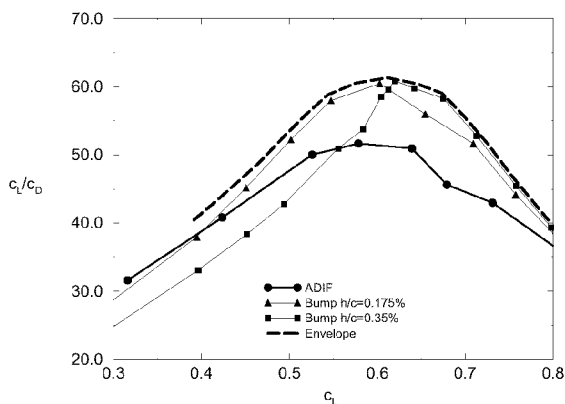
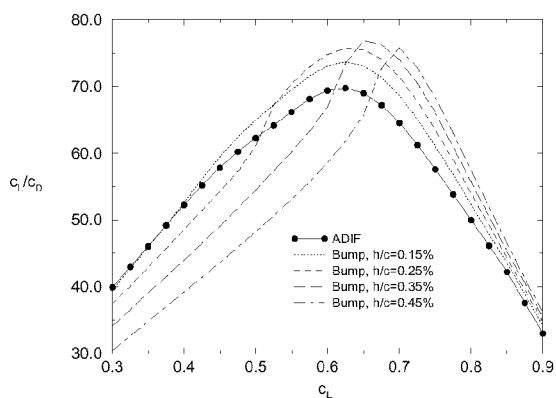
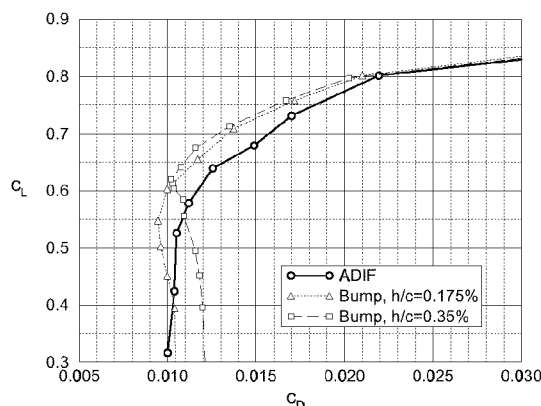
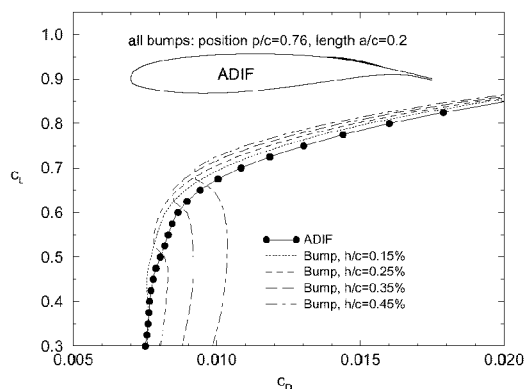


Figure 6: Calculated drag and lift-over-drag ratio for the ADIF airfoil for different bump heights at $M = 0.755$

Figure 8: Measured drag and lift-over-drag ratio for the ADIF airfoil for different bump heights at $M = 0.765$

Figure 6 shows the computed lift polars and the L/D ratios for a Mach number slightly above the airfoil design Mach number and different bump heights. It can be seen clearly, that higher bumps reach their maximum performance at higher lift coefficients, whereas they produce additional drag at low lift coefficients due to unfavorable double shock configurations such as shown in Fig 5. To obtain the best results over the whole polar the bump therefore has to be adaptive, also adjusting its position which for the sake of simplicity was fixed for these examples. The benefits can be exploited in terms of a higher maximum of the L/D ratio for these off-design conditions as well as a wider usable range of lift coefficients with a given (minimum) L/D value.

The numerical results in Fig. 5 and Fig. 6 were confirmed by experimental data obtained in the Cryogenic Ludwig Tube of DLR in Göttingen, given in Fig. 7 and Fig. 8. The model was equipped with two exchangeable inserts with bump heights of 0.175% and 0.35% chord, respectively. The pressure distribution in the shock region in Fig. 7 as well as the polars and L/D ratios in Fig. 8 show the same trends as the numerical results. The maximum drag reduction for this Mach number was obtained with about 24% for the bump with a height of 0.35% chord.

4 SHOCK CONTROL ON A SWEEPED WING BY CONTOUR BUMPS, PERFORATION AND SUCTION

To find out, whether the results of the 2-d airfoil investigations do also apply for a swept wing, where the boundary layer is three-dimensional and the shock/boundary layer interaction might respond differently to these control devices, a model of a swept wing was designed and built for the 1 m x 1 m TWG, Ref. 3. The swept wing design was chosen because a half model would not have been large enough in this wind tunnel to accommodate the different inserts. Contoured liners were necessary on the side walls of the test section to ensure infinite sweep conditions, see Fig. 9.

The test results showed that the effect of the flow control devices was in principle not very different from the 2-d case. Figure 10 shows an example of a pressure distribution in the shock region and Fig. 11 the polars for the swept wing equipped with a bump of 0.16% chord height with and without additional suction upstream of the shock.

There was basically no drag reduction achievable from the passive ventilation. The bumps showed a somewhat smaller drag

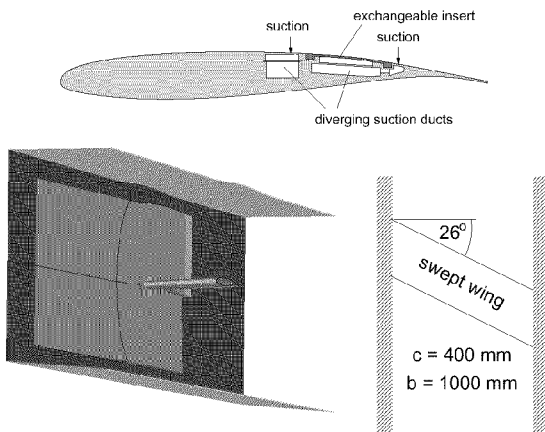


Figure 9: The ADIF swept wing model for shock control applications

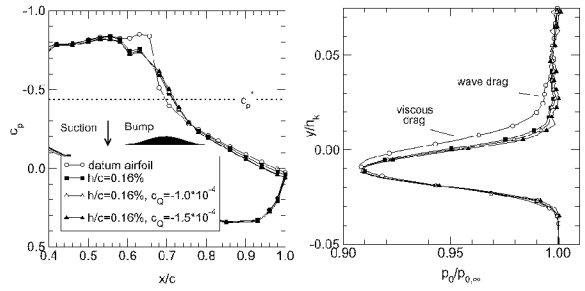


Figure 10: Pressure distribution in the shock region of the ADIF swept wing with and without bumps and boundary layer suction at $M = 0.852$

reduction as on the airfoil tests, cf. Fig. 11, this is however believed to be in part caused by a premature boundary layer transition leading to comparatively higher boundary layer thicknesses as in the 2-d experiment. The addition of boundary layer suction upstream of the shock reduces the boundary layer thickness again and leads to higher drag reductions and probably these values are to be compared with the 2-d results.

5 APPLICATION OF CONTOUR BUMPS IN COMBINATION WITH VARIABLE CAMBER

Modern wing designs will utilize variable camber to optimize aerodynamic performance for different flight conditions. For transonic speed one effect of variable camber is also to reduce wave drag by redistributing the pressure such that strong shocks are avoided. Therefore it was to be investigated, whether additional benefits may still be gained by a combination of variable camber and the contour bump for shock control.

A numerical optimization study was performed employing variable camber, here realized in form of a flexible trailing edge, together with a contour bump. For each lift coefficient, the optimum combination of trailing edge deflection, bump position and height for minimum drag was determined. An example of the results is given in Fig. 12.

For the Mach number chosen for this test case, the variable camber is most efficient for low values of the lift coefficient, whereas at high lift the bump achieves higher drag reductions. The combination of both devices gives a significantly better performance than either one alone. This balance changes with Mach number. In general, the contour bump is most effective at high Mach

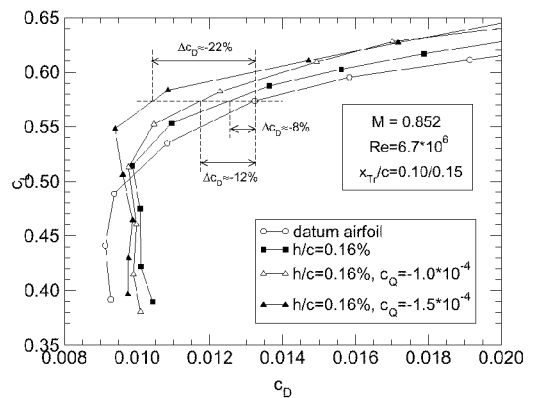


Figure 11: Drag polars for the ADIF swept wing with and without bumps and boundary layer suction

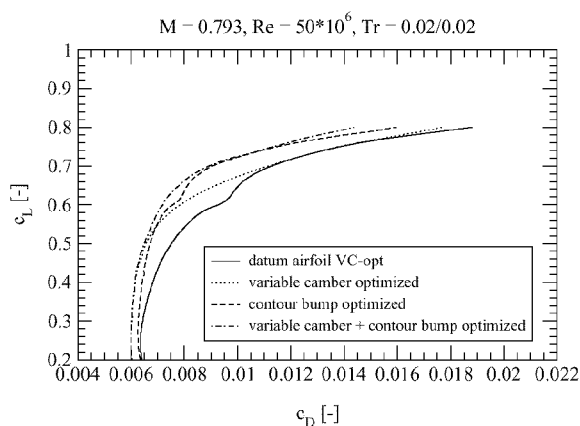


Figure 12: Drag polar for the VC-opt airfoil with optimized trailing edge deflection and bump

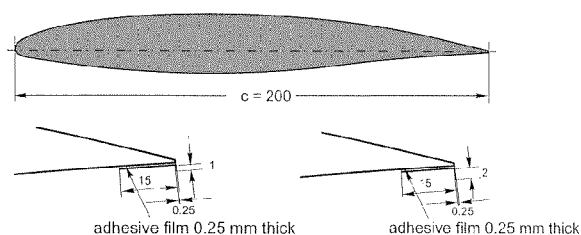


Figure 13: CAST-10 airfoil with 0.5% and 1% chord Gurney flaps

numbers/high lift coefficients, where the effect of the flap is not sufficient to eliminate wave drag.

A similar effect as with flexible trailing edges and flaps can be achieved with small trailing edge modifications like Gurney flaps. Two configurations on a CAST-10 airfoil were investigated experimentally in the 1 m x 1 m TWG, cf. Fig. 13.

The two pressure distributions in Fig. 14 at about the same lift coefficient explain, why in the drag polars in Fig. 15 the configurations with Gurney flaps develop a better performance at high lift coefficients. The re-distribution of the pressure reduces low pressures on the suction side of the airfoil, such that a shock is no longer formed and wave drag is avoided. Further investigations on trailing edge modifications to enhance aerodynamic performance at transonic speed with very small devices are planned.

6 SUMMARY AND CONCLUSION

Flow control by passive ventilation, contour bumps and trailing edge devices has been investigated both numerically and experimentally at transonic speed in the region of the drag rise. All these devices is in common, that they achieve most of their potential of drag reduction by minimizing wave drag, either by direct interaction with the shock, like the ventilation and the bump, or by changing the pressure distribution such that strong shocks are no longer necessary because the maximum velocities on the suction side of the airfoil are greatly reduced.

Total drag reductions can not be achieved by passive ventilation, since the reduction of wave drag is more than outweighed by an increase in viscous drag due to the losses in the flow through the perforation.

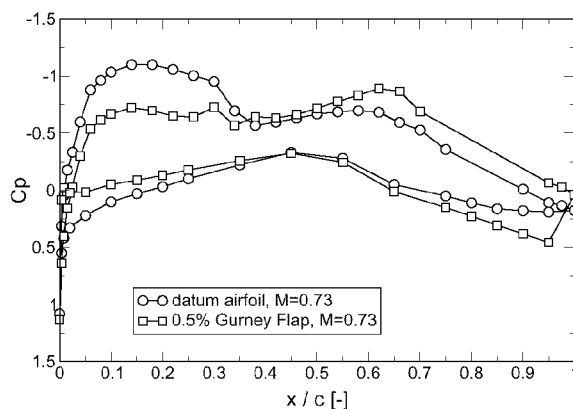


Figure 14: Pressure distribution for the CAST-10 airfoil with and without 0.5% chord Gurney flap

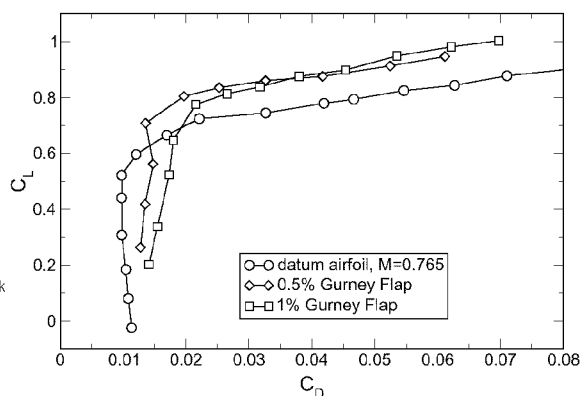


Figure 15: Drag polars for the CAST-10 airfoil with 0.5% and 1% chord Gurney flaps at $M = 0.765$

The contour bump is very effective in reducing wave drag at off-design conditions, especially at high Mach numbers and high lift coefficients. A maximum of 24% drag reduction could be achieved. Flexible trailing edges or flaps have similar benefits, but at lower Mach numbers and lift coefficients. By combining these two devices the drag polar for high Mach numbers can be enhanced over the whole range of lift coefficients.

Small trailing edge devices like Gurney flaps show promising results also in the transonic regime. Their potential for drag reduction will be subject to further studies.

REFERENCES

1. R. Bur, J. Délery, and B. Corbel. Basic study of passive control applied to a two-dimensional transonic interaction. In E. Stanewsky, J. Délery, J. Fulker, and W. Geißler, editors, *EUROSHOCK — Drag Reduction by Passive Shock Control*, pages 355 – 378. Vieweg, 1997.
2. H. Rosemann. The Cryogenic Ludwig-Tube at Göttingen. In *Special Course on Advances in Cryogenic Wind Tunnel Technology*, AGARD-R-812, DLR, (Cologne, Germany), 20–24 May 1996.
3. J. Birkemeyer. Widerstandsminimierung für den transsonischen Flügel durch Ventilation und adaptive Konturbeule. DLR Forschungsbericht FB 99-28, DLR, 1999.
4. A. Knauer. Die Leistungsverbesserung transsonischer Profile durch Konturmodifikationen im Stoßbereich. DLR

Forschungsbericht FB 98-03, DLR, 1998.

5. H. Rosemann, A. Knauer, and E. Stanewsky. Experimental investigation of the transonic airfoils DA LVA-1A and VA-2 with shock control. In E. Stanewsky, J. Délery, J. Fulker, and W. Geißler, editors, *EUROSHOCK — Drag Reduction by Passive Shock Control*, pages 355 – 378. Vieweg, 1997.

Paper #16

Q by Chris Weir: The predicted benefit will be of great interest to the airframe companies and the airlines. When do you believe that the technology might enter service ?

A : The technology requires a new wing design. No prediction is given.